ISSN 1064-2293, Eurasian Soil Science, 2020, Vol. 53, No. 10, pp. 1455–1468. © Pleiades Publishing, Ltd., 2020.
Russian Text © The Author(s), 2020, published in Pochvovedenie, 2020, No. 10, pp. 1247–1261.

SOIL BIOLOGY

Free Iron and Iron-Reducing Microorganisms in Permafrost and Permafrost-Affected Soils of Northeastern Siberia

E. M. Rivkina[a, *], D. G. Fedorov-Davydov[a], A. G. Zakharyuk[b], V. A. Shcherbakova[b], and T. A. Vishnivetskaya[a, c]

[a] *Institute of Physicochemical and Biological Problems of Soil Science, Russian Academy of Sciences, Pushchino, Moscow oblast, 142290 Russia*

[b] *Skryabin Institute of Biochemistry and Physiology of Microorganisms, Russian Academy of Sciences, Pushchino, Moscow oblast, 142290 Russia*

[c] *University of Tennessee, 1416 Circle Drive, Knoxville, TN 37996-1605 USA*

**e-mail: rivkina@issp.psn.ru*

Received March 4, 2020; revised March 21, 2020; accepted March 27, 2020

Abstract—An agreement between the content of amorphous (oxalate-extractable) iron and morphochromatic features of gley attests to the modern activity of gleyzation processes in tundra soils of the Kolyma Lowland, especially within lower parts of gentle and steep slopes. A suprapermafrost reduced gley horizon thawing out in the warmest years is considered a relic of the warmer and wetter stage of soil formation. An integrated analysis of data on the contents of mobile iron and annotated metagenomes indicates that microorganisms affiliated with the Proteobacteria phylum capable of iron reduction predominate in sediments formed under hydromorphic conditions and in modern mineral soil. In laboratory experiments, the process of microbial iron reduction was more active at 5°C than at 20°C. Therefore, it can be assumed that the majority of cultivated communities of iron-reducing bacteria have been adapted to low Arctic temperatures. Under conditions of climate warming and an increase in precipitation, permafrost temperature, and thickness of the seasonally thawed layer, iron reduction processes in the soils rich in the total iron will play an even greater role and create favorable redox conditions for the formation of methane, one of the most important greenhouse gases.

Keywords: iron, metagenome, microorganisms, iron reduction

DOI: 10.1134/S1064229320100166

INTRODUCTION

The processes of microbiological reduction of iron, as well as sulfate reduction and denitrification, play an important role in the organic matter transformation and establishment of favorable redox conditions for the formation of methane, one of the most important greenhouse gases. Climate changes in the recent decades have caused an increase in the active layer thickness and permafrost temperature below the depth of zero annual temperature amplitude in the subarctic regions [9, 10, 14], which should lead to the activation of biological processes.

Ferrous iron in soils and bottom sediments is the source of electrons for iron-oxidizing microorganisms, whereas Fe (III) can work as the final acceptor of electrons for iron reducers [13, 25, 27]. The ratio between Fe (III) and Fe (II) is indicative of the conditions of formation and cryopreservation of sediments in subarctic regions. It was found that concentrations of ferrous iron are higher than those of ferric iron in permafrost sediments and soils, whose development took place mainly under hydromorphic conditions [6, 7]. The relationship between concentrations of Fe (II) and methane in lacustrine, lacustrine–alluvial, and marine deposits of the Holocene and Pleistocene ages was demonstrated in these studies. It is known that microbiological processes of iron reduction, as well as denitrification and sulfate reduction, create favorable redox conditions for the terminal anaerobic process—biogenic methane formation.

We demonstrated earlier that the bacteria, which can reduce Fe (III) to Fe (II) under incubation temperature of 15°C, preserve their viability in the 7 to 10 ka-old Holocene permafrost (alas) deposits [19]. The number of iron reducers reached 2×10^3 cells/g at concentration of ferrous iron 0.008–0.027 g/100 g soil. Viable iron-reducing bacteria were not found in the underlying Pliocene–Lower Pleistocene deposits of the Olyor suite (more than 600 ka in age) despite a much higher content of Fe (II): from 0.156 to 0.240 g/100 g soil. Psychroactive sulfate reducers *Desulfovibrio arcticus* [18] and *Desulfovibrio gilichinskyi* [21] capable of reducing Fe (III) without visible growth of these bacteria were isolated from cryopegs—

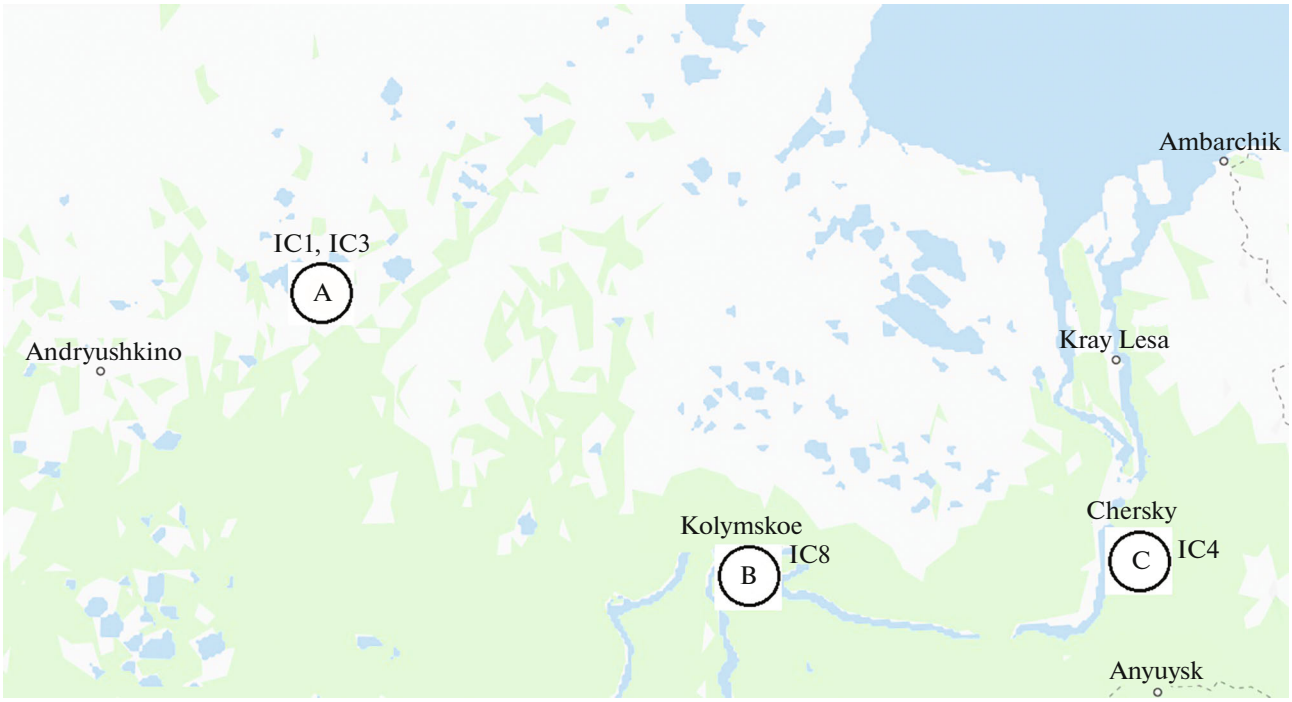

Fig. 1. Studied sites: (A) Alazeya River, (B) Omolon River mouth, and (C) Ambolikha River (Google maps).

hypersaline interlayers with unfrozen water—in permafrost of the Varandei and Yamal peninsulas. However, the cultures of psychrophilic and psychroactive bacteria capable of utilizing ferric iron as a source of energy for growth were not isolated from permafrost.

Theoretical and experimental data [12] indicate that direct reduction of iron oxides without preliminary dissolution of Fe (III)-containing compounds is a widespread process in nature. However, under laboratory conditions, iron reducers more often utilize dissolved compounds of ferric iron, such as Fe (III) citrate and Fe (III) EDTA, as electron acceptors. It was shown that members of the *Shewanella*, *Geobacter*, and *Aeromonas* genera could perform the reduction reaction directly on the surfaces of iron-containing minerals due to position of iron reductase enzyme in outer membrane of these bacteria.

Single representatives of the *Shewanella*, *Geobacter*, *Desulfuromonas,* and *Desulfuromusa* genera [11, 24] capable of iron reduction at temperature about 4°C were isolated recently form marine deposits of the Arctic. The members of Geobacteraceae family are able to reduce Fe (III) via oxidation of acetate and other organic substrates to carbon dioxide.

The goal of our study was to describe the processes of the formation of ferrous iron in modern tundra soils and permafrost. The following tasks were solved:

(a) the assessment of the content and distribution of nonsilicate iron, including its mobile form, in tundra soils and underlying permafrost;

(b) the analysis of the results of comparative metagenome analysis of the modern tundra soil and three samples of the Late Pleistocene permafrost sediments aimed at identification of the genes that encode proteins and enzymes participating in the iron cycle and the 16S rRNA genes of bacteria participating in the process of iron reduction; and

(c) the study of the microbial reduction of iron under laboratory conditions.

OBJECTS AND METHODS

Objects of the Study

Field studies were performed on a key site in the western part of the Kolyma Lowland, in the middle reaches of the Alazeya River near the northern boundary of the taiga zone; this area is included in Olyor zone of neotectonic uplift (Fig. 1a). The thickness of the yedoma sediments at this site does not exceed 10–20 m. Pliocene–Lower Pleistocene lacustrine-alluvial loamy deposits of the Olyor suite are found below the Yedoma suite in the section and are underlain by the Late Neogene epicryogenic sands of the Tumus-Yar suite. The presence of small thermoerosional cirques on steep slopes of yedoma outliers attests to their continuous destruction.

Zonal vegetation on the watersheds is represented by dwarf-shrub–herbaceous–green-moss associations. Hillocky microtopography and active formation of frost boils predetermine the soil cover structure.

The content of nonsilicate iron was studied in soils of three catenas on a steep (25°–30°) slope of northern exposure, gentle (7°–15°) slope of northern exposure, and on a gentle slope of southern exposure in the basin of the Alazeya River. Additionally, core samples were taken from boreholes at three geographical points: in the Alazeya River basin (Al3-15 and 2-98), on the bank of the Ambolikha River (a channel of the Kolyma River) (4-07), and in the Omolon River mouth (2-07). Borehole 4-07 on the bank of the Ambolikha River penetrated frozen sediments of an oxbow lake formed 34 ka ago [20] and underlain by coarse sands of the Begunov suite. Deposits penetrated by borehole 2-07 in the area of the Omolon River mouth were represented by the Late Pleistocene loams of the ice complex.

To determine the genes and proteins of microorganisms participating in iron reduction, metagenomes were obtained and the microbiological study was carried out.

METHODS OF THE STUDY

Borehole drilling and core sampling were performed with an UKB 12/25 driller without blowing or mud flushing in compliance with the requirements of sterility as described earlier [22].

Soil samples to determine nonsilicate iron were taken from the main horizons of soil profiles under sodded hillocks and from frozen bottom of the sections. In the case of section 518-07, samples from the frozen layer were taken to the depth of 15 cm from the base of seasonally thawed layer; below, pure ice of apparently polygonal ice-wedge nature was found.

Loss on ignition, pH, extractable acidity, and the contents of exchangeable cations and CO_2 of carbonates were determined in the Chemical Laboratory of the Institute of Physicochemical and Biological Problems of Soil Science, Russian Academy of Sciences. Total carbon was determined by dry combustion in the Common Use Center of the Laboratory of Radiocarbon Dating and Electron Microscopy, Institute of Geography, Russian Academy of Sciences. The content of organic carbon was calculated as the difference between the total carbon content and the content of the carbon of carbonates determined by the acidimetric analysis.

Determination of iron. Fractional composition of nonsilicate iron was determined according to Zonn's scheme [3] in the Laboratory of the Department of Geography and Evolution of Soils, Institute of Geography, Russian Academy of Sciences. Concentrations of mobile forms of iron extracted with 0.1 N sulfuric acid from the fresh samples were determined in the field [1]. Similar determination of mobile iron in the samples of permafrost deposits was carried out in the laboratory, to where core samples were delivered in the frozen state. Mobile iron was determined using the method developed for natural water [5] with separate titration of trivalent and bivalent forms with 0.01 N Trilon B. Concentrations of trivalent iron were determined under laboratory conditions via titration, and concentrations of bivalent iron were determined by colorimetric analysis with 0.5% solution of α,α-dipyridyl according to the Virigina–Arinushkina method (GOST 27395-87). For soils of steep northern slope (sections 508-07, 509-07, and 510-07), where concentrations of oxalate-extractable and acid-extractable iron in fresh samples were determined in the same profiles, we can say exactly, which part of the total content of amorphous iron is represented by mobile (acid-extractable) form. As for the soils sampled on the watersheds and gentle slopes, corresponding analyses were performed for the soils of different catenas, so we can only approximately estimate the fraction of mobile iron in them.

Molecular methods. A PowerSoil® kit (MO BIO Laboratories Inc., USA) was used to isolate the total DNA from the samples of soils and frozen sediments; purification and concentration of the obtained DNA was carried out using the Genomic DNA Clean and Concentrator® kit (Zymo Research Corporation, USA). Sequencing of metagenomes was performed in the Centre for Genomic Regulation, Barcelona, Spain, with the use of an Illumina HiSeq 2000™ platform and in the University of Tennessee (USA) with the use of an Illumina MiSeq platform. Untreated data on sequencing (about 19.8 Gb, i.e., 143.7–150.0 million sequences with the mean length of 150 pairs of bases) were uploaded to the MG-RAST server [16] for obtaining genome annotations. More than 95% of sequences met quality control standards.

Microbiological methods. To obtain enrichment culture of iron-reducing bacteria, we used modified medium [29], to which the solutions of microelements [23] (1.0 mL/L), vitamins [28] (10.0 mL/L), and yeast extract "Difco" (0.002 g/L) were added. Sodium acetate (final concentration 20 mM) was used as a source of carbon and donor of electrons, and Fe (III) citrate (final concentration 10 mM) was used as an acceptor of electrons. Mineral medium was prepared and microorganisms were cultivated in strictly anaerobic conditions under N_2 (100% in gas phase) atmosphere and at pH 7.0–7.2. The cultures were incubated under darkroom conditions at 5 and 20°C during 40 days. Mineral medium without inoculation was used as a chemical control. Reduction of Fe (III) was determined using colorimetric method by the formation of stabile colored complex of ferrous iron with ferrozine [26].

RESULTS AND DISCUSSION

The morphology and chemical properties of studied soils. Soils of the key plot in the Alazeya River basin (Fig. 1a) have a silty loamy or clay loamy texture and are characterized by the absence of the eluvial-illuvial differentiation. The presence of humus tongues in the upper part of the profiles and cryoturbation inclusions of peat in the middle and lower parts of the profiles

due to cryoturbation are typical of the soils on elevated elements of the microrelief. The best-drained positions on the divide and upper parts of gentle slopes are occupied by suprapermafrost gleyic cryozems. Within the middle part of a gentle slope of northern aspect and within the lower parts of a gentle slope of southern aspect and a steep slope of northern aspect, cryozems are replaced by cryoturbated gleyzems. Raw-humus (AO) or mucky (H) horizons are typical of the upper parts of soil profiles on the slopes. On the top of the divide with intense development of frost boils, such horizons do not have enough time for development, and the upper organo-accumulative part of the profile is often represented by the peaty weakly developed humus horizon (Wт). The upper and middle-profile mineral horizons of cryozems are represented by nongleyed or slightly gleyed horizons (Bhi, Bcrm, B@, etc.); gley features become more pronounced in the lower part of the profile in the gleyic Bg horizon. In the lowermost part of the profiles of cryozems, immediately above the permafrost table (50–70 cm), the gley horizon (Gт) is present; this horizon thaws out from permafrost in the warmest summer seasons. It is characterized by the bluish gray or bluish color with rare yellow or ocherous stains, high moisture content, often thixotropy, abrupt transition from the overlying gleyic horizons, absence of structure, dense consistence, high humus content, and the presence of subhorizontal peat lenses and interlayers (up to two–four) lying parallel to one another. Cryozems and gleyzems differ in the ratio between nongleyed and gleyed parts of the profile. Nongleyed horizons occupy a half or two thirds of the active layer in cryozems; in gleyzems, their thickness decreases; in gleyzems forming at the foot of slopes, it does not exceed 3–6 cm.

Strongly acid reaction (Table 1) is typical of the upper soil horizons on the watersheds; deeper, the reaction becomes moderately acid. The extractable acidity decreases down the soil profiles from 6–19 to 2–3 cmol/kg, and base saturation of soil adsorption complex (**SAC**) increases from 25–46% to 68–80%. Soils of gentle slopes are characterized by strongly acid reaction in the entire profile, except for the moderately acid deep gley horizon. Base saturation increases down the soil profiles from 25–30% to 52–73%. Calcium predominates in the composition of exchangeable bases in these soils, as well as in the soils of local divides. Soils of steep slopes are characterized by domination of moderately acid reaction, which can be replaced by slightly acid reaction in the lower parts of soil profiles and by neutral reaction in the gley horizon. Base saturation of SAC is low only in organic horizons and reaches 61–96% in mineral horizons. Calcium and magnesium predominate in the composition of exchangeable bases.

Distribution of iron forms in soil profiles. The accumulative distribution of total nonsilicate (dithionite-extractable) iron is mainly observed in soils of slopes, and the accumulative distribution of crystallized form of nonsilicate iron is observed in all cases. This distribution pattern is predetermined by the biogenic accumulation of iron in the upper part of soil profiles and its removal from the lower part, especially from the suprapermafrost horizon, under the impact of gleyzation. The mean weighted content of dithionite-extractable iron in soil profiles on gentle slopes ranges within 1.90–2.10%.

The content of amorphous (oxalate-extractable) iron usually has the bimodal distribution with a minimum in the middle-profile horizons. The share of amorphous iron in nonsilicate iron increases in the lower gleyic horizons and, especially, in the gley horizon. Abrupt widening of the ratio between concentrations of oxalate- and dithionite-extractable iron ($[Fe_{ox}]/[Fe_{dt}]$, Schwertmann coefficient) in mineral horizons is observed in the soils of steep slope, for which the values of this coefficient increase down the soil profile from 0.37–0.42 to 0.72–0.93. The Schwertmann coefficient in soils of gentle slopes does not differ so significantly between the upper and lower mineral horizons: 0.34–0.37 and 0.49–0.59, respectively. An increase in this coefficient down the soil profile from 0.47 to 0.83, i.e., close to that in the soils of steep slope, is observed at the footslope positions. The values of Schwertmann coefficient in organo-accumulative horizons are relatively small (0.37–0.61), and this can be due to low temperatures favoring dehydration and crystallization of amorphous iron compounds in the upper part of soil profiles. In the lower parts of both gentle and steep slopes (sections 507-07 and 510-07), where optimal conditions are formed for snow accumulation, this coefficient in the organo-accumulative horizon (0.51–0.61) is significantly higher than that in the soils of other positions (0.37–0.44). The contents of pyrophosphate-extractable iron (Bascomb's procedure) are high (0.47–0.81%) in the organic horizons and decrease to 0.07–0.33% in the mineral horizons.

Small accumulation of dithionite-extractable iron in organo-accumulative horizons and an increase in its content down the soil profiles in the mineral layer followed by a sharp decrease in the suprapermafrost horizon is observed in the soil of local divide (section 502-07). The mean weighted content of dithionite-extractable iron in this soil profile reaches 1.89%. The distribution of oxalate-extractable iron repeats the distribution of dithionite-extractable iron, but has a smoother pattern. The accumulation of nonsilicate iron in the weakly developed peaty humus horizon (Wт) and a decrease in its content in the suprapermafrost horizon are not so pronounced in the soil of the divide. The values of Schwertmann coefficient vary within a narrow range (from 0.43 to 0.53) and sharply increase in the gley horizon (up to 0.86). Pyrophosphate-extractable iron has a bimodal distribution with maximums in the horizons with the high content of organic matter (Tables 1, 2), i.e., in the upper organ-accumulative horizon and in the suprapermafrost gley horizon. In

Table 1. Chemical properties of tundra soils in the Alazeya River basin

Horizon	Depth, cm	C_{org}, %	pH		Total acidity, cmol/kg	Exchangeable bases, cmol/kg				Base saturation, %
			H_2O	KCl		Ca	Mg	Na	K	
Pit 502-07, local divide										
Wт	0–4	12.52	4.2	3.6	18.80	5.62	4.38	0.35	0.85	24.78
Bhi	4–8	Nd	4.9	3.8	6.30	4.72	4.28	0.42	0.49	46.19
B	8–17	1.47	5.8	4.7	2.70	6.96	4.90	0.36	0.26	70.83
B@	17–36	1.23	6.0	4.9	2.00	9.66	4.94	0.30	0.30	79.81
Bg1	36–41	1.19	5.9	4.8	2.08	6.88	4.68	0.26	0.37	75.47
Bg2	41–51	1.94	5.7	4.6	2.96	6.94	4.40	0.29	0.46	68.46
Gт	51–64	3.15	5.5	4.4	4.09	6.96	3.90	0.27	0.59	60.58
Pit 504-07, middle part of a gentle slope of southern aspect										
AO	0–4	13.59	4.3	3.5	19.81	6.26	4.12	0.63	0.75	24.90
Bcrm	4–7	Nd	4.7	3.5	6.71	4.50	2.90	0.23	0.33	38.85
B@	7–21	1.61	5.3	4.1	3.89	5.30	4.06	0.22	0.28	57.11
Bg_1	23–30	1.21	5.4	4.3	2.93	4.88	3.80	0.25	0.21	62.08
Bg_2	30–46	1.76	Nd	Nd	2.76	6.56	4.24	0.28	0.29	68.43
Gт	58–64	4.60	5.5	4.6	4.47	9.02	4.14	0.27	0.44	61.97
Pit 507-07, lower part of a gentle slope of southern aspect										
AO	0–6	14.36	4.2	3.3	19.96	5.48	3.92	0.54	0.77	23.16
Bcrm	6–9	1.32	5.2	4.0	3.8	4.78	3.66	0.20	0.30	55.38
Bg_2	18–36	1.52	5.3	4.0	3.92	6.10	3.62	0.22	0.20	57.35
Bg_3	38–50	2.26	5.3	4.2	5.06	6.18	3.86	0.32	0.25	52.44
Gт	51–59	1.41	5.8	4.9	1.90	6.32	3.06	0.20	0.36	73.40
Pit 508-07, upper part of a steep slope of northern aspect										
H	0–2	8.71	5.2	4.5	17.98	7.66	7.42	0.39	1.44	34.28
Bcrm	3–6	Nd	5.5	4.5	2.16	4.58	4.44	0.29	0.42	70.78
B@	6–14	0.96	5.7	4.8	2.05	5.24	4.40	0.31	0.27	72.48
Bg_1	14–35	0.79	5.9	4.8	1.74	5.56	4.40	0.23	0.23	75.74
Bg_2	22–45	1.66	6.0	5.1	1.95	6.78	3.20	0.22	0.28	73.85
Bg_3	45–60	Nd	6.2	5.3	1.22	5.46	4.06	0.24	0.29	81.20
Gт	60–69	0.27	7.0	6.1	0.20	5.12	3.90	0.23	0.30	96.13

* Nd, not determined.

these horizons, the share of humus-bound iron reaches almost a half of the total content of amorphous iron. The content of pyrophosphate-extractable iron generally increases downward through the mineral part of the soil profile (Fig. 2).

An increase in the content of oxalate-extractable iron, mainly in the gleyic horizons, takes place down the studied catena, i.e., in the direction of an increase in morphochromatic characteristics of gleyzation. A higher content of pyrophosphate-extractable iron is seen in the soil on the lower part of the gentle slope in comparison with the soil of the divide because of an increase in the percentage of organic-bound iron in amorphous Fe_2O_3.

The mean weighted content of nonsilicate (dithionite-extractable) iron in the soil profiles on steep slope reaches 1.57, 1.67, and 1.78% for sections 508-07, 509-07, and 510-07, respectively; on the average, it is 15% lower than in the soils of the divide and gentle slopes. A decrease in the content of nonsilicate iron in the soils on steep slope in comparison with the soils of the divide takes place at the expense of amorphous iron in the upper nongleyed part of the soil profiles and at the expense of both amorphous and crystallized forms of iron in the gleyed horizons. A tendency for redistribution of nonsilicate iron, mainly its oxalate-extractable form, along the studied catena is observed against the background of a general loss of iron from

Table 2. Fractional composition of nonsilicate iron in tundra soils of the Alazeya River basin, % per ignited soil

Horizons	Depth, cm	Fe						Schwertmann coefficient
		dithionite-extractable	crystallized	total amorphous (oxalate-extractable)	amorphous organic-bound (pyrophosphate-extractable)	amorphous mineral	mobile (acid-extractable)	
Pit 502-07, top of local divide								
Wт	0–4	1.33	0.65	0.68	0.34	0.34	Nd	0.51
B	8–17	1.13	0.53	0.60	0.11	0.49	″	0.53
B@	17–36	1.56	0.88	0.68	0.11	0.57	″	0.43
Bg_1	36–41	1.70	0.92	0.78	0.12	0.66	″	0.46
Bg_2	41–51	1.84	0.88	0.98	0.17	0.81	″	0.53
Gт	51–64	0.80	0.11	0.69	0.36	0.33	″	0.86
Pit 504-07, middle part of a gentle slope of southern aspect								
AO	0–4	1.90	1.20	0.70	Nd	Nd	Nd	0.37
B@	7–21	1.41	0.89	0.52	″	″	″	0.37
Bg_1	23–30	1.29	0.83	0.46	″	″	″	0.36
Bg_2	30–46	1.34	0.73	0.61	″	″	″	0.46
Gт	58–64	1.36	0.69	0.67	″	″	″	0.49
Pit 505-07, lower part of a gentle slope of southern aspect								
Wт	0–3	1.51	0.90	0.61	Nd	Nd	Nd	0.40
B	5–15	1.59	1.05	0.54	″	″	″	0.34
Bg_2	15–20	1.49	0.92	0.57	″	″	″	0.38
Bg_3	21–47	1.61	0.95	0.66	″	″	″	0.41
Gт	47–57	1.07	0.44	0.63	″	″	″	0.59
Pit 507-07, lower part of a gentle slope of southern aspect								
AO	0–6	1.74	0.86	0.88	0.56	0.32	Nd	0.51
Bcrm	6–9	1.32	0.70	0.62	0.17	0.45	″	0.47
Bg_2	18–36	1.47	0.75	0.72	0.18	0.54	″	0.49
Bg_3	38–50	1.23	0.54	0.69	0.23	0.46	″	0.56
Gт	51–59	0.76	0.13	0.63	0.22	0.41	″	0.83
Pit 508-07, upper part of a steep slope of northern aspect								
AO	0–5	1.36	0.85	0.51	Nd	Nd	Nd	0.37
G	2–14	1.77	0.99	0.78	″	″	0.335	0.44
B@	6–14	1.10	0.73	0.37	″	″	0.031	0.34
Bg_1	14–35	0.95	0.57	0.38	″	″	0.043	0.40
Bg_2	22–47	1.14	0.63	0.51	″	″	0.027	0.45
Gт	55–69	0.69	0.05	0.64	″	″	0.043	0.93
Pit 509-07, middle part of a steep slope of northern aspect								
AO	0–5	1.54	0.96	0.58	Nd	Nd	Nd	0.37
B@	9–14	1.28	0.75	0.53	″	″	0.015	0.41
Bg_1	14–35	1.12	0.70	0.42	″	″	0.047	0.38
Bg_2	35–57	1.17	0.70	0.47	″	″	0.045	0.40
Gт	62–74	0.93	0.24	0.69	″	″	0.712	0.74
Pit510-07, lower part of a steep slope of northern aspect								
AO	2–6	1.67	0.66	1.01	Nd	Nd	0.242	0.61
B@	11–28	1.21	0.70	0.51	″	″	0.048	0.42
Bg	32–41	1.24	0.27	0.97	″	″	0.228	0.79
Gт	41–53	1.07	0.29	0.78	″	″	0.553	0.72

* Nd, not determined.

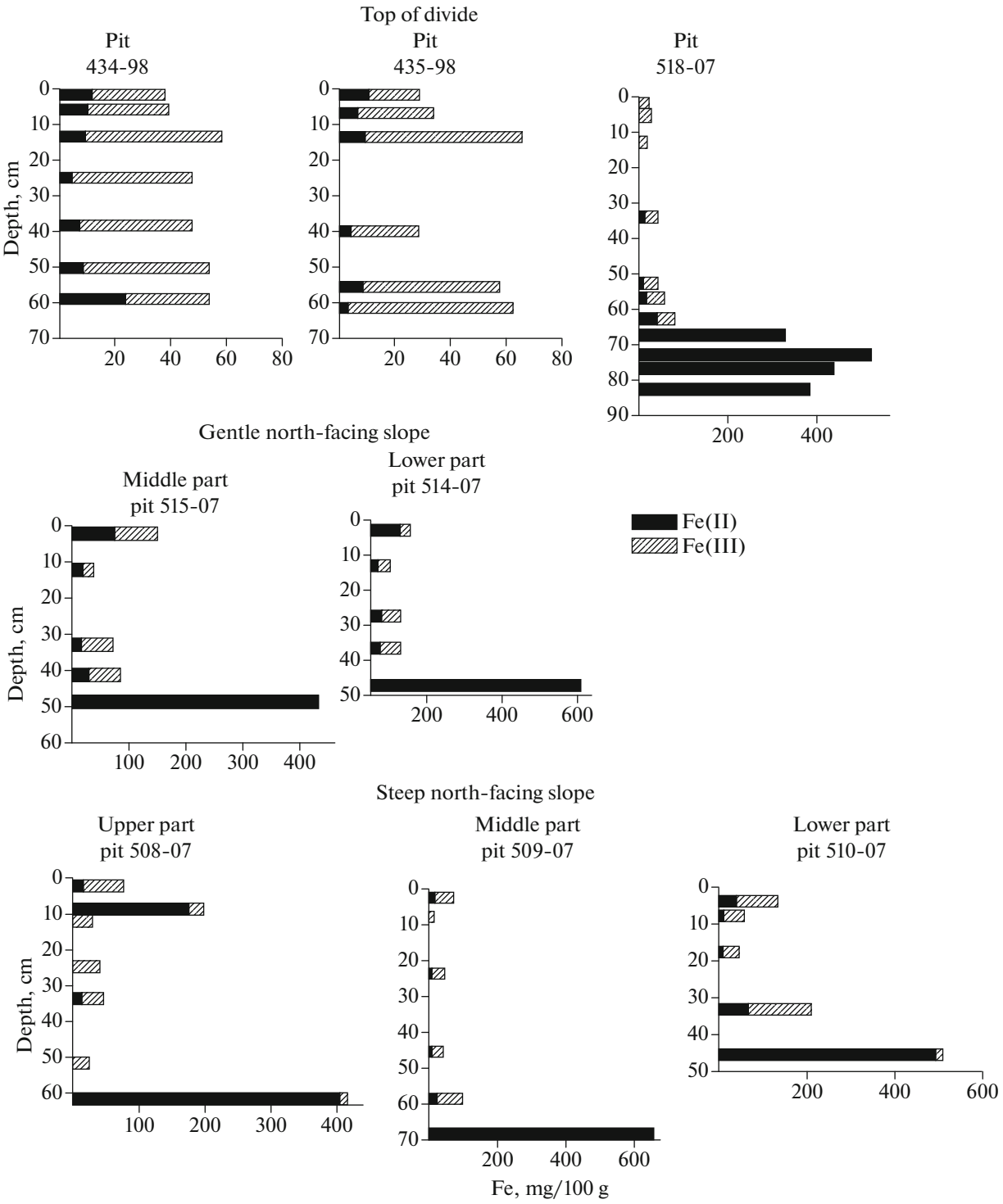

Fig. 2. Mobile iron in tundra soils.

the soils of steep slopes. Thus, the soils on the upper and middle parts of steep slopes are most impoverished in nonsilicate iron. The ratio between amorphous and crystallized iron changes in the lower part of the slope, and the Schwertmann coefficient increases to 0.42–0.79.

The content of mobile iron extracted with 0.1 N H_2SO_4 from the fresh samples has a bimodal distribution in the soils of slopes (Fig. 2). The upper maximum is in the mucky or raw-humus horizons (71–148 mg Fe/100 g soil); in section 508-07, it is observed in the horizon of with surface gleyzation (stagnic features)

and reaches 197 mg Fe/100 g soil. The lower maximum is much higher (417–659 mg Fe/100 g soil) and corresponds to the suprapermafrost gley horizon. Additionally, iron extractability changes significantly upon transition from the upper mineral Bhi, Bcrm, B@, and other horizons to the lower gleyic Bg horizon and sharply increases in the gley (Gт) horizon, where extractable iron is mainly present in the bivalent form. An increase in the content of acid-extractable iron down the soil profiles agrees well with more pronounced manifestation of the morphochromatic characteristics of iron mobility. The [Fe (II)]/[Fe (III)] ratio in the upper part of the soil profiles can be slightly wider due to the participation of bivalent iron in the undecomposed plant tissues. It reaches maximum values (>1.00) in the surface-gleyed horizon (section 508-07), in the raw-humus AO horizon (section 514-07), and in the mucky H horizon (section 515-07). It varies within a wide range (0.08–0.90) in the mineral horizons and tends to infinity in the gleyed suprapermafrost horizon.

The percentage of acid-extractable iron in oxalate-extractable iron in mineral horizons slightly increases down the soil profiles and sharply increases in the gley horizon. It is about 17–29% in the organo-accumulative horizons, 43% in the surface-gleyed horizon, 3–10% in the nongleyed mineral horizons, 5–24% in the gleyic mineral horizons, and 67–100% in the suprapermafrost gley horizons. In the latter case, all amorphous iron in some soil profiles is represented by mobile compounds of Fe (II). The distribution of acid-extractable iron in soils of the divide differs from that in soils of the slopes in the absence of the upper maximum due to the specificity of organo-accumulative horizons mostly represented by weakly developed humus horizons. An increase in the content of acid-extractable iron down the soil profile on the divide is smoother than that in the soils of slopes. The content of mobile iron in the frozen part of the gley horizon is even higher than that in the thawed part. The [Fe (II)]/[Fe (III)] ratio ranges within 0.10–0.60 in the nongleyed mineral horizons and within 0.18–1.13 in the gleyic mineral horizons. The fraction of acid-extractable iron in oxalate-extractable iron in these horizons reaches approximately 4–12 and 52–83%, respectively.

An increase in the content of acid-extractable iron is in agreement with a more pronounced morphological manifestation of gley features down the soil profiles both on gentle and steep slopes. The differences between the particular soils of the studied catenas are seen in the participation of bivalent and trivalent forms of iron (with a predominance of bivalent iron in all the soils, especially on gentle slopes). In the gleyed suprapermafrost horizons, virtually all mobile (acid-extractable) iron is in the bivalent form.

The correspondence between an increase in the content of acid-extractable iron down the soil profiles, as well as down the catenas, and a simultaneous increase in the morphochromatic features of gleyzation is an argument in favor of the hypothesis about the modern nature of this process in the studied soils. Despite the predominance of oxidizing conditions in the soils on drained watersheds, gleyzation plays a significant role in them and should be included in the complex of soil-forming processes.

Gleyzation becomes a dominant process in the lower parts of gentle slopes because of their greater moistening. The contents of oxalate-extractable and acid-extractable iron and the fraction of ferrous form in the latter increase in the soils from the upper to the lower positions in mesotopography. In the same direction, the pH values and the degree of base saturation decrease, and the potential acidity increases.

Soils of steep slopes develop under the conditions of continuous sheet erosion, which specifies their youth. They are characterized by colder tints of background color and lower acidity, which in this case can be considered an indicator of the degree of pedogenic alteration of parent material. The soil reaction in lower horizons can be close to neutral or neutral. A lower content of dithionite-extractable iron in the soils of steep slopes in comparison with the soils of level watersheds and gentle slopes can be due to the removal of mobile iron compounds that are present in significant amounts in the Yedoma and, especially, Olyor deposits. Oxalate- and acid-extractable iron is also redistributed within the slope, especially in its lower part. These soils are subjected to continuous water inflow due to melting of shallow-lying ice wedges, so that the conditions of strong waterlogging are developed in the steep slopes, and the most gleyed soils are formed. The same type of catenas was described by us earlier on Cape Medvezhii [8].

Gley horizon in the suprapermafrost part of most of the described soils is the most interesting and difficult for interpretation object. In addition to its morphological specificity, this horizon is also characterized by the significant loss of total nonsilicate and crystallized iron, predomination of amorphous iron over crystallized iron, the high content of complex iron–organic compounds and of mobile (acid-extractable) iron in oxalate-extractable iron, and absolute predominance of bivalent iron among mobile iron compounds. These features are indicative of the stability of reducing conditions. The high content of water-soluble and exchangeable Fe (II) has been confirmed by intense qualitative reaction with α,α-dipyridyl under natural conditions.

At the same time, a discrepancy between the presence of reduced gley horizon and mesophilic tundra vegetation, especially on drained watersheds and upper parts of gentle slopes, a abrupt transition to the Gт horizon from the overlying gleyic horizon, and preservation of the lower part of the gley horizon in the permafrost allow us to suppose that this horizon has a relic nature. Its widespread distribution attests to the

fact that its age is no greater than the age of recent mesorelief. It can be supposed that the Gт horizon is genetically related to organic-accumulative suprapermafrost horizon described in the tundra zone of the Kolyma Lowland [2, 4]. The latter is included into this gley horizon, and we suggest that they should be considered as a single whole.

As demonstrated by our studies in the Alazeya River basin (since 1998) and in the Kolyma Lowland in general (since 1984), the gley horizon can remain in the frozen state below the layer of seasonal thawing and the activity of modern pedogenetic processes for years, and probably for decades. Irregular and short-time thawing of the lower part of this horizon may lead to certain transformation of its upper part with changes in the color pattern, appearance of yellow-ocherous stains, and the formation of oxidized gley horizon (Gox) above the gley horizon (sections 434-98 and 435-98); this may also result in a lower content of acid-extractable iron in the periodically thawing part of the Gт horizon in comparison with its permanently frozen part. However, there is no complete oxidative degradation of the thawing part of the gley horizon. One of the reasons for its high redox buffering may be related to the inclusions of considerable masses of the peat material into this horizon owing to cryoturbation.

A comparison of iron extractability with 0.1 N H_2SO_4 determined in cold 1998 and warm 2007 on the adjacent watersheds demonstrated that an increase in the thickness of the active layer and the thawed part of the gley horizon changed the distribution pattern of mobile iron in the soil profile with a general increase in its storage in the soil and with changes in the ratio between ferrous and ferric forms (Fig. 2).

Distribution of iron forms in permafrost. The content of mobile iron in the upper part of geological section of permafrost of the Yedoma suite (borehole Al 3-15) at the key plot of the Alazeya River basin varies within a broad range. Gray and bluish gray horizons enriched in mobile iron (185–1432 mg Fe/100 g) mainly represented by ferrous form alternate with horizons of uneven color and relatively low mobile iron content (39–138 mg Fe/100 g) with a predominance of ferric iron (the [Fe (II)]/[Fe (III)] ratio is 0.08–0.38). In most cases, this ratio in permafrost is higher than that in the surface soils, except for their suprapermafrost gley horizon. Underlying deposits of the alluvial Olyor suite sampled in borehole 2-98 are characterized by a very high extractability of iron (up to 2366–2865 mg Fe/100 g) and by the virtual absence of its ferric form. This attests to the domination of reducing conditions in these deposits.

Determination of ferrous and ferric iron in core samples of permafrost from boreholes 2-07 and 4-07 indicates the prevalence of Fe (II) over Fe (III) in both cases; ferric iron is almost absent in the Holocene floodplain sediments and in the Late Pleistocene sediments of an oxbow lake (borehole 4-07) and is present in small amounts in sediments of the Yedoma suite (ice complex) (Fig. 3). The presence of biogenic methane was detected in all the samples from this borehole, whereas it was not found in borehole 2-07 [20]. The predominance of ferrous form over ferric form of mobile iron in most of the permafrost samples indicates the domination of the process of iron reduction and allows us to assume the presence of iron-reducing bacteria and specific enzymes related to their activity in the microbial communities of permafrost.

Analysis of metagenomes. Metagenomic analysis is one of the most informative methods to assess the diversity of natural microbial communities. This approach also allows us to evaluate the functional genes of proteins responsible for the main biogeochemical processes. The analysis of annotated metagenomes indicates that the predominance of nine bacterial and one archaeal phyla: Proteobacteria, Actinobacteria, Firmicutes, Chloroflexi, Bacteroidetes, Acidobacteria, Cyanobacteria, Verrucomicrobia, Planctomycetes, and Euryarchaeota (Fig. 4). The number of microorganisms belonging to other phyla does not exceed 1%. The genes of microorganisms belonging to the Proteobacteria phylum predominate in the samples of frozen sediments of an oxbow lake (IC4) and in the gleyic Bg horizon (50–60 cm) of the suprapermafrost gleyic heavy loamy cryozem (IC1). Actinobacteria are most widely present in the Late Pleistocene yedoma sediments sampled in boreholes 2-07 and Al3-15 (samples IC8 and IC3). It is known that most of iron-reducing bacteria belong to Proteobacteria phylum [15]. We found that sample IC4 (frozen sediments of an oxbow lake) contains more microorganisms related to the methane cycle than sample IC8 (frozen yedoma sediments) [20]. The analysis of four metagenomes made it possible to compare the numbers of 16S rRNA gene sequences belonging to three major genes of iron-reducing bacteria: *Shewanella*, *Geobacter,* and *Desulfuromonas* (Fig. 5a). In frozen sediments of an oxbow lake (sample IC4) and in gleyic horizon of modern tundra soil (sample IC1), these microorganisms are represented by a greater number of genes 16S rRNA than that in the ice complex (samples IC8 and IC3).

It is known that all living organisms, including bacteria, require iron. This element enters the composition of proteins performing the most important metabolic functions. Genes that encode proteins participating in assimilative and dissimilative processes of iron reduction and oxidation have been identified in the studied metagenomes (Table 4). It can be seen that proteins responsible for the processes of iron cycle, including iron transport into microbial cell, predominate in sample IC1 (gleyic horizon of modern tundra soil); their participation in sample IC3 (frozen yedoma sediments) is lower. A comparison of proteins in samples IC4 and IC8 indicates that the set of proteins necessary for iron reduction is represented by a larger number of copies in IC4 than in IC8, whereas proteins of assimilative iron reduction are represented

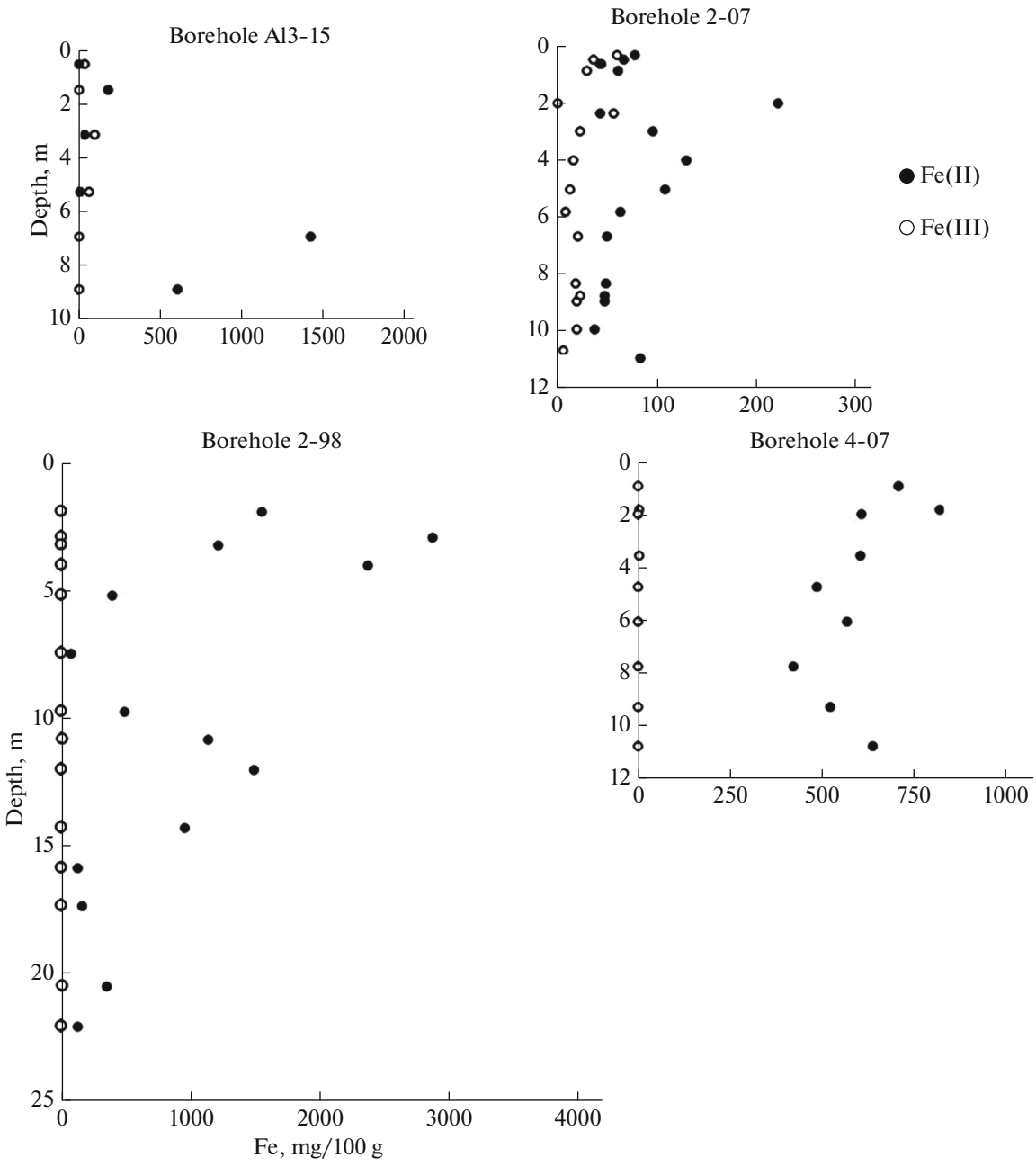

Fig. 3. Mobile iron in boreholes.

by a greater number of genes in IC8 than in IC4. These data confirm the high potential of biogeochemical reactions performed by microorganisms in the course of the formation of soils and sedimentary deposits.

Microbiological study. Enrichment cultures, in which the process of ferric iron reduction took place at different temperatures of cultivation, were obtained from the samples of borehole 4-07 in the area of the Ambolikha River. The quantity of reduced iron ranged within 0.5–2.21 mM in enrichment cultures incubated at 20°C (Fig. 5b). The maximum content of Fe (II) ions (2.21 mM) was found in enrichment culture M5 obtained from the permafrost sample at the depth of 22.2–22.3 m in the Kolyma Lowland, and the minimum Fe (II) content (<0.5 mM) was detected in enrichment culture M2 obtained from the depth of 1.4 m. The content of Fe (II) ions reached 0.67 mM in enrichment culture M4 obtained from the depth of 17.5–17.6 m of the same borehole.

The content of Fe (II) ions ranged from 0.79 to 2.70 mM in enrichment cultures incubated at 5°C for 40 days. Microbial communities of three enrichment

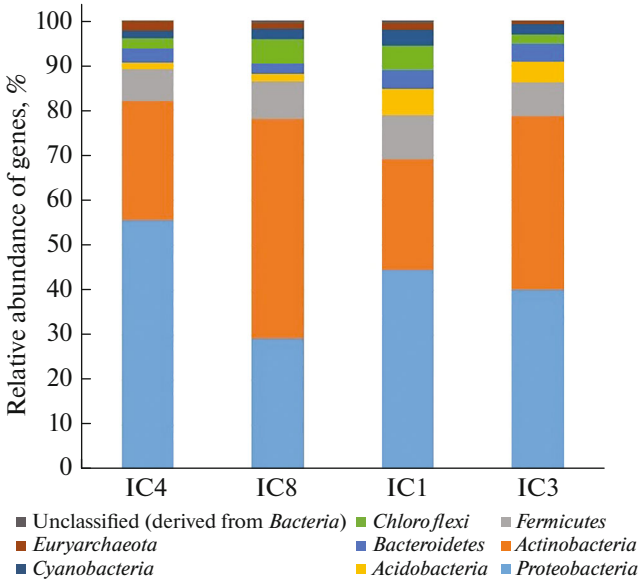

Fig. 4. Analysis of metagenomes at the phylum level (normalized data). Only the phyla with the relative participation of more than 1% are shown.

cultures reduced Fe (III) citrate with the formation of maximum amounts of Fe (II) in the course of their growth. The maximum content of Fe (II) (2.70 mM) was found in enrichment culture M5 obtained from the permafrost sample in the Kolyma Lowland. The content of reduced iron was 1.65 mM in enrichment culture M4 obtained from the permafrost at the depth of 17.5–17.6 m in the same borehole.

The results of experiments with enrichment cultures demonstrated that the communities of iron-reducing bacteria obtained from different samples and cultivated at 5°C were more efficient iron reducers than the communities from the same samples cultivated at 20°C. In 2017, our foreign colleagues [17] found that the rate of iron reduction in enrichment cultures obtained from subglacial deposits taken in different geographically remote area was higher at the cultivation temperature of 4°C in comparison with 15°C.

CONCLUSIONS

The data obtained in our study attest to the possibility of modern gleyzation process in the soils of divides and slopes under conditions of the continental climate of tundra zone in the Kolyma Lowland. In the soils forming in the lower parts of gentle and steep slopes, gleyzation is a predominant process.

The gley horizon (Gт) periodically thawing out from permafrost in the warmest years is characterized by predomination of the ferrous form of mobile iron in the composition of nonsilicate iron, which favors the loss of iron from this horizon. It can be supposed that the studied horizon is a relic of a warmer and wetter stage of pedogenesis in the past. Despite some transformation of the upper part of the gley horizon upon its thawing, no complete oxidative degradation of this horizon takes place; partly, this may be due to the buffering role of peaty interlayers and lenses included in the Gт horizon in the course of cryoturbation.

The genes of microorganisms responsible for iron reduction have been identified on the basis of the analysis of genome annotations. It is shown that the phy-

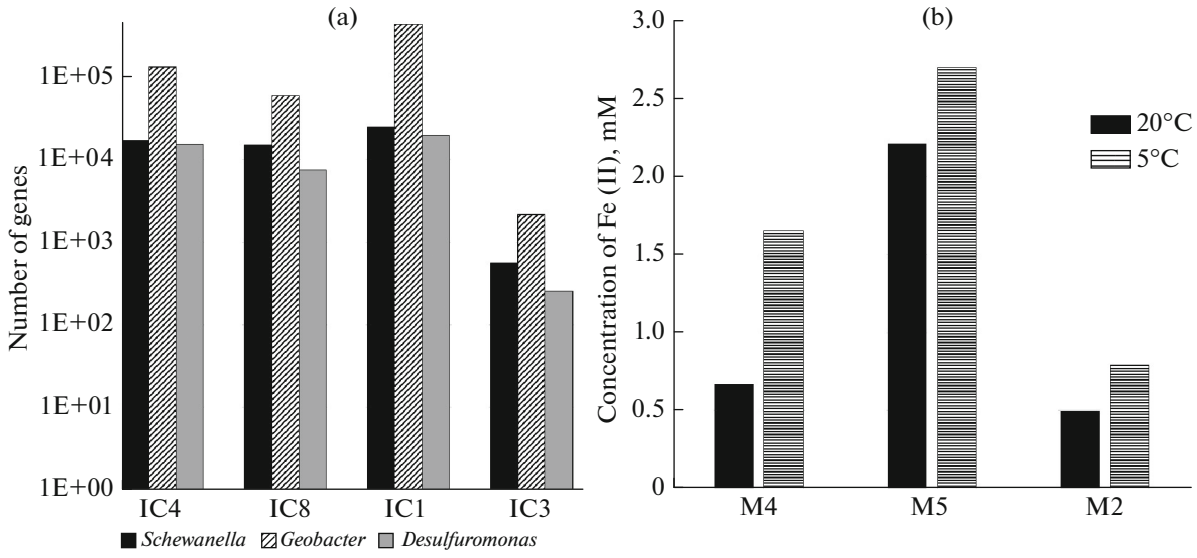

Fig. 5. (a) Number of 16S rRNA genes of iron-reducing microorganisms and (b) formation of ferrous iron in enrichment cultures incubated at different temperatures. The samples represented in Fig. 5b were taken from borehole 4-07 (Ambolikha River) (Fig. IC4, Table 3) from the depths of 1.4 m (M2), 17 m (M4), and 22 m (M5).

Table 3. Places of sampling for microbiological and metagenomic study

Sample	Study area	Location and borehole number	Depth, m	Description
IC1	A (69.338869° N, 154.996948° E)	Alazeya River	0.5–0.6	Recent soil (suprapermafrost-gleyish heavy loamy cryozem, horizon Bg)
IC3		Alazeya River, borehole Al3-15	3.5	Peaty horizon in Late Pleistocene glacial complex
IC8	B (68.693947° N, 158.710142° E)	Omolon River, borehole 2-2007	16	Glacial complex, Late Pleistocene, loam
IC4	C (68.711290° N, 161.434493° E)	Ambolikha River, borehole 4-2007	1.4 17.5 22.0	Bayou lake, Late Pleistocene, loam

Location of key areas A, B, and C is indicated in Fig. 1.

Table 4. Functional proteins associated with iron cycle (number of protein-encoding genes in metagenomes of modern soils and permafrost)

Nomenclature	Functional proteins	Alazeya River		Ambolikha River and Omolon River	
		IC1	IC3 (Al3-15)	IC4 (4-07)	IC8 (2-07)
	Fe-containing proteins				
EC 1.2.7.1	Pyruvate: ferredoxin oxidoreductase	27291	155	9588	1858
EC 1.2.7.8	Indolepyruvate oxidoreductase	15875	159	18473	2051
EC 1.2.7.4*	Carbon monoxide dehydrogenase	195098	1479	51839	51725
EC 1.17.1.9*	Formate dehydrogenase–O, iron–sulfur	2066	11	798	278
EC 1.18.1.3	Naphthalene 1,2–dioxygenase system ferredoxin–NAD(+) reductase	17	1	16	68
EC	4Fe–4S ferredoxin, iron–sulfur binding	12623	7	10511	7212
EC 1.7.7.1	Ferredoxin—nitrite reductase	2874	22	584	108
EC 1.18.1.2	Ferredoxin—NADP(+) reductase	3118	1	1531	310
EC 1.8.7.1	Ferredoxin—sulfite reductase (assimilatory)	6842	35	919	858
	Proteins of assimilative iron reduction				
EC 1.5.1.30	Flavin reductase	588	21	958	420
EC 7.1.1.8*	Ubiquinol–cytochrome c reductase	26319	858	20376	23046
EC	Ferredoxin, 2Fe–2S	26660	142	2667	4219
	Proteins of dissimilative iron reduction				
	Periplasmic decaheme cytochrome c, Mtr A, D	1567	5	75	40
EC 1.18.6.1	Nitrogenase (molybdenum–iron)	2810	19	1380	22
EC 1.18.6.1	Nitrogenase (vanadium–iron)	4	9	7	0
	Proteins of Fe (III) and Fe (II) transport				
EC 4.99.1.1	Ferrochelatase, protoheme ferro–lyase	32978	690	15682	13913
	Ferrous iron transport protein B	56840	380	14643	2605
	Proteins regulated transport of Fe (III) and Fe (II)				
	Ferric uptake regulation protein FUR	19736	120	2526	975

lum Proteobacteria containing iron-reducing microorganisms predominates in the gleyic horizon of the interfluve soil. Three genera—*Shewanella* (the class of Gammaproteobacteria) and *Geobacter* and *Desulfuromonas* (Deltaproteobacteria)—are widely present in these samples.

The process of microbial reduction in the incubated samples from frozen sediments of an oxbow lake (IC4) takes place, and its activity is higher under incubation temperature of 5°C than under 20°C. It can be assumed that the major part of cultivated communities of iron-reducing bacteria in the studied samples is well adapted to the low temperatures of permafrost in the Arctic region. Such psychrophilic communities play an important role in the iron cycle and organic matter destruction in cold ecosystems.

It is demonstrated that iron reduction and microorganisms participating in it are an important factor of the formation of redox conditions in the Late Pleistocene sediments and modern soils in the studied region. It can be assumed that all biochemical processes, including iron reduction, will play an even more important role in local ecosystems upon climate warming, increase in atmospheric precipitation, higher permafrost temperature, and greater thickness of the seasonally thawed (active) layer.

ACKNOWLEDGMENTS

We are grateful to A.V. Lupachev for assistance in carrying out field researches.

FUNDING

This study was performed within the framework of state assignment no. AAAA-A18-118013190181-6 and was supported by the Russian Foundation for Basic Research (project nos. 19-29-05003-mk and 19-04-00831) and, partly, by the National Science Foundation (grant NSF DEB-1442262).

CONFLICT OF INTEREST

The authors declare that they have no conflict of interest.

REFERENCES

1. E. V. Arinushkina, *Manual for the Chemical Analyses of Soils* (Moscow State Univ., Moscow, 1970) [in Russian].
2. S. V. Gubin and A. V. Lupachev, "Suprapermafrost horizons of the accumulation of raw organic matter in tundra cryozems of Northern Yakutia," Eurasian Soil Sci. **51**, 772–781 (2018).
3. Z. V. Zonn, *Iron in Soils: Genetic and Geographical Aspects* (Nauka, Moscow, 1982) [in Russian].
4. A. V. Lupachev and S. V. Gubin, "Suprapermafrost organic–accumulative horizons in the tundra cryozems of Northern Yakutia," Eurasian Soil Sci. **45**, 45–55 (2012).
5. E. P. Mulikovskaya, A. A. Reznikov, and I. Yu. Sokolov, *Analysis of Natural Waters* (Nedra, Moscow, 1970) [in Russian].
6. E. M. Rivkina, G. N. Kraev, K. V. Krivushin, K. S. Laurinavizhyus, D. G. Fedorov-Davydov, A. L. Kholodov, V. A. Shcherbakova, and D. A. Gilichinskii, "Methane in permafrost of the northeastern sector of Arctic," Kriosfera Zemli **10** (3), 23–41 (2006).
7. D. G. Fedorov-Davydov, S. V. Gubin, and O. V. Makeev, "The content of mobile iron and gleyzation process in soils of the Kolyma Lowland," Eurasian Soil Sci. **37**, 131–142 (2004).
8. D. G. Fedorov-Davydov, N. S. Mergelov, and M. M. Morozov, "Soil cover of the Kolyma Lowland coastal yedomas," in *Proceedings of the International Conference "Cryogenic Resources of Polar Regions," Salekhard, June, 2007* (Salekhard, 2007), Vol. 2, pp. 113–116.
9. D. G. Fedorov-Davydov, S. P. Davydov, A. I. Davydova, V. E. Ostroumov, A. L. Kholodov, V. A. Sorokovikov, and D. G. Shmelev, "Temperature regime of soils of Northern Yakutia," Kriosfera Zemli **22** (4), 15–24 (2018).
10. A. Abramov, S. Davydov, A. Ivashchenko, D. Karelin, A. Kholodov, G. Kraev, A. Lupachev, et al., "Two decades of active layer thickness monitoring in northeastern Asia," Polar Geogr., 1–17 (2019). https://doi.org/10.1080/1088937X.2019.1648581
11. J. P. Bowman, S. A. McCammon, D. S. Nichols, J. H. Skerratt, S. M. Rea, P. D. Nichols, and T. A. McMeekin, "*Shewanella gelidimarina* sp. nov., *Shewanella frigidimarina* sp. nov., novel Antarctic species with the ability to produce eicosapentaenoic acid (20: 5ω3) and grow anaerobically by dissimilatory Fe (III) reduction," Int. J. Syst. Evol. Microbiol. **47** (4), 1040–1047 (2005).
12. D. Canfield, E. Kristensen, and B. Thamdrup, *Aquatic Geomicrobiology* (Elsevier, Amsterdam, 2005), Vol. 48. ISBN 9780080575407
13. R. E. Cowart, "Reduction of iron by extracellular iron reductases: implications for microbial iron acquisition," Arch. Biochem. Biophys. **2**, 273–281 (2002). https://doi.org/10.1016/S0003–9861(02)00012-7
14. D. G. Fyodorov-Davydov, A. L. Kholodov, V. E. Ostroumov, G. N. Kraev, V. A. Sorokovikov, S. P. Davydov, and A. A. Merekalova, "Seasonal thaw of soils in the North Yakutian ecosystems," in *Proceedings of the Ninth International Conference on Permafrost, University of Alaska, Fairbanks, June 29–July 3, 2008* (Fairbanks, 2008), Vol. 1, pp. 481–486.
15. S. Hedrich, M. Schlömann, and D. B. Johnson, "The iron-oxidizing proteobacteria," Microbiology **157** (6), 1551–1564 (2011). https://doi.org/10.1099/mic.0.045344-0
16. F. Meyer, D. Paarmann, M. D'Souza, R. Olson, E. M. Glass, M. Kubal, T. Paczian, A. Rodriguez, R. Stevens, A. Wilke, and J. Wilkening, "The metagenomics RAST server–a public resource for the automatic phylogenetic and functional analysis of metagenomes," BMC Bioinf. **9**, 386 (2008). https://bmcbioinformatics.biomedcentral.com/articles/10.1186/1471–2105–9–386
17. S. L. Nixon, J. P. Telling, J. L. Wadham, and C. S. Cockel, "Viable cold-tolerant iron-reducing microorganisms

in geographically diverse subglacial environments," Biogeosciences **14** (6), 1445–1455 (2017). https://doi.org/10.5194/bg-14-1445-2017

18. S. A. Pecheritsyn, E. M. Rivkina, V. N. Akimov, and V. A. Shcherbakova, "*Desulfovibrio arcticus* sp. nov., a psychrotolerant sulphate-reducing bacterium from a cryopeg," Int. J. Syst. Evol. Microbiol. **62** (1), 33–37 (2012). https://doi.org/10.1099/ijs.0.021451–0
19. E. Rivkina, D. Gilichinsky, S. Wagener, J. Tiedje, and J. McGrath, "Biogeochemical activity of anaerobic microorganisms from buried permafrost sediments," Geomicrobiol. J. **15** (3), 187–193 (1998). https://doi.org/10.1080/01490459809378075
20. E. Rivkina, L. Petrovskaya, T. Vishnivetskaya, K. Krivushin, L. Shmakova, M. Tutukina, A. Meyers, and F. Kondrashov, "Metagenomic analyses of the late Pleistocene permafrost-additional tools for reconstruction of environmental conditions," Biogeosciences **13** (7), 2207–2219 (2016). https://doi.org/10.5194/bg-13-2207-2016
21. Y. Ryzhmanova, T. Abashina, D. Petrova, and V. Shcherbakova, "*Desulfovibrio gilichinskyi* sp. nov., a cold-adapted sulfate-reducing bacterium from a Yamal Peninsula cryopeg," Int. J. Syst. Evol. Microbiol. **69** (4), 1081–1086 (2019). https://doi.org/10.1099/ijsem.0.003272
22. T. Shi, R. H. Reeves, D. A. Gilichinsky, and E. I. Friedmann, "Characterization of viable bacteria from Siberian permafrost by 16S rDNA sequencing," Microb. Ecol. **33** (3), 169–179 (1997).
23. A. I. Slobodkin and J. Wiegel, "Fe (III) as an electron acceptor for H_2 oxidation in thermophilic anaerobic enrichment cultures from geothermal areas," Extremophiles **1** (2), 106–109 (1997).
24. V. Vandieken, M. Mussmann, H. Niemann, and B. B. Jørgensen, "*Desulfuromonas svalbardensis* sp. nov., *Desulfuromusa ferrireducens* sp. nov., psychrophilic, Fe (III)–reducing bacteria isolated from Arctic sediments, Svalbard," Int. J. Syst. Evol. Microbiol. **56** (5), 1133–1139 (2006). https://doi.org/10.1099/ijs.0.63639-0
25. B. A. Ventura, F. González, A. Ballester, M. L. Blázquez, and J. A. Muñoz, "Bioreduction of iron compounds by *Aeromonas hydrophila*," Int. Biodeter. Biodegrad. **103**, 69–76 (2015). https://doi.org/10.1016/j.ibiod.2015.03.034
26. E. Viollier, P. W. Inglett, K. Hunter, A. N. Roychoudhury, and P. van Cappellen, "The ferrozine method revisited: Fe(II)/Fe(III) determination in natural waters," Appl. Geochem. **15** (6), 785–790 (2000). https://doi.org/10.1016/S0883-2927(99)00097-9
27. K. A. Weber, L. A. Achenbach, and J. D. Coates, "Microorganisms pumping iron: anaerobic microbial iron oxidation and reduction," Nat. Rev. Microbiol. **4** (10), 752–764 (2006). https://doi.org/10.1038/nrmicro1490
28. E. A. Wolin, M. Wolin, and R. S. Wolfe, "Formation of methane by bacterial extracts," J. Biol. Chem. **238** (8), 2882–2886 (1963).
29. C. Zhang, R. D. Stapleton, J. Zhou, A. V. Palumbo, and T. J. Phelps, "Iron reduction by psychrotrophic enrichment cultures," FEMS Microbiol. Ecol. **30** (4), 367–371 (1999). https://doi.org/10.1111/j.1574-6941.1999.tb00664.x

Translated by T. Chicheva